On the Parameter Estimation for the Discrete-Element Method in LS-DYNA®

Nils Karajan[1], Zhidong Han[2], Hailong Teng[2], Jason Wang[2]
[1]DYNAmore GmbH, Industriestraße 2, 70569 Stuttgart, Germany
[2]Livermore Software Technology Corporation,
7374 Las Positas Rd., Livermore, CA 94551, United States

Abstract

The goal of this contribution is to discuss the assumptions made when modeling granular media with the discrete-element method (DEM). Herein, particular focus is drawn on the physical interpretation of the involved material parameters of the DEM in LS-DYNA®. Following this, the influence of each parameter on the bulk behavior of granular media is investigated and different possibilities to estimate these parameters are presented.

Granular Media

The umbrella term "granular media" follows the simple idea to characterize materials consisting of discrete particles but embraces a relatively complex class of materials, whose bulk behavior strongly depends on the length scale, the grain surface characteristics as well as the grain-size distribution. In particular, typical engineering problems may range from particle sizes as small as 1 µm to as big as 1 m and even more, cf. Figure 1.

Fig. 1: Different length scales for particle sizes [all images taken from wikipedia.org].

Note that the driving forces may change on the respective length scale as the surface-to-volume ratio changes, i.e., the ratio increases as the radius of the particles decreases. Following this, particle assemblies on small scales are often "surface driven" by adhesion, etc., while large scale particles are "volume-driven" by gravity. An example for "equal forces" can be found in sand castles where the adhesion of the wetted sand is in the range of the gravitational forces pulling at the sand grains.

Moreover, besides the size of the particles, their shape is also of great influence. While Figure 1 shows many examples with rather spherical particles, Figure 2 depicts particles of arbitrary shape. Herein, non-spherical particles have the characteristic to introduce additional moments due to the possible offset of contact forces. In LS-DYNA, non-spherical particles are currently under development. At this stage, non-spherical particles need to be approximated by defining a rolling friction to account for the additional moment.

Fig. 2: Different particle shapes [all images taken from wikipedia.org].

Finally, granular media are also known as materials with internal friction. The consequence in combination with the above is a complex bulk behavior, which depends on the kind of motion the material undergoes. In particular, granular media may exhibit three different kinds of material behavior:

- Solid-like behavior when compacted
  - Static friction law is not violated
  - Load is carried by grain-to-grain contact forces
- Fluid-like behavior when in motion
  - Static friction law is violated
  - Motion is induced by rolling/slipping
- "Simple" Newtonian motion for separated particles

Note that all three behaviors may occur simultaneously but at different positions of conveyor belts or similar engineering systems. This is why it is extremely important to determine the parameters dominating each of the three behaviors.

The Discrete-Element Method in LS-DYNA

For the sake of this contribution, only the most important keywords will be briefly reviewed. More detailed information on the implementation of the DEM in LS-DYNA can be found in the latest draft version of the LS-DYNA manual or in Karajan et al. [1].

In LS-DYNA, the DEM is realized using rigid spherical particles in accordance to Cundall & Strack [2]. The DEM computes the motion of each spherical particle using Newton's law of motion and thus, each particle may have three displacements and three rotations as degrees of freedom. As usual for the DEM, a penalty-based contact is used to capture the particle-particle (and particle-wall) interaction of dry and wet particles, cf. Figure 3a.

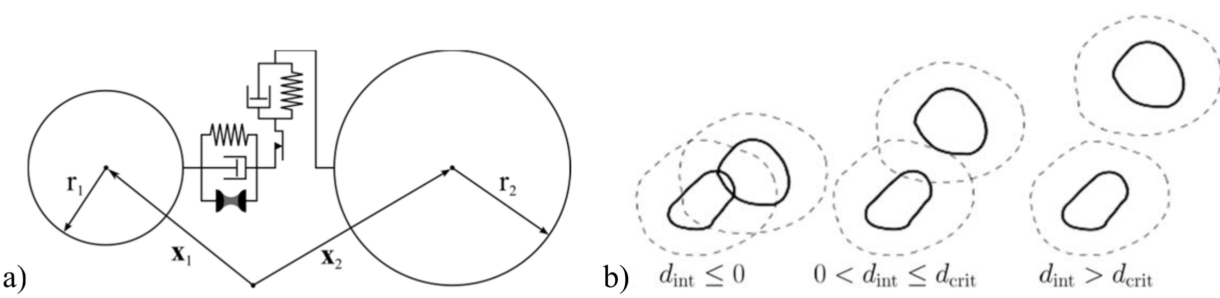

Fig. 3: a) Penalty-based particle-particle interaction in LS-DYNA and b) possible collision states for mechanical contact, liquid-bridge activity for wet particles and free motion, respectively.

Figure 3b shows three different collision states that can be distinguished depending on the interaction distance d_{int} between adjacent particles

$$d_{\text{int}} = r_1 + r_2 - |\mathbf{x}_1 - \mathbf{x}_2|. \tag{1}$$

The first case describes the mechanical contact situation between two rigid particles, where small overlaps (penetrations) may occur due to the penalty formulation of the contact. In the case of wet particles, the liquid surface tension of the wetting agent may lead to so-called liquid bridges that cause an attracting force between adjacent particles. In the last cast, particles are free to go and keep their momentum until another collision is detected.

Definition of the Spherical Particles

Associated keywords

The particles are defined using the keyword **`*ELEMENT_DISCRETE_SPHERE_OPTION`**, which requires the initial coordinate of each sphere to be given via the node ID of **`*NODE`** as well as its respective radius. The missing values for mass *M* and inertia *I* need to be computed and prescribed for each particle using

$$M = V\rho = \frac{4}{3}\pi r^3 \rho \qquad \text{and} \qquad I = \frac{2}{5} M r^2 = \frac{8}{15}\pi r^5 \rho\,. \tag{2}$$

If the option **`*ELEMENT_DISCRETE_SPHERE_VOLUME`** is used, the values for mass and inertia need to be prescribed using a normalized density of $\rho = 1$, whereas the actually applied density of the particles is taken from **`*MAT_ELASTIC`** to scale the prescribed values of mass and inertia internally in LS-DYNA according to (2).

Associated parameters

First of all, there is the need to define the radius together with either the discrete particle mass or the density of the granular material. Depending on what a single particle is representing, the density is usually either the real or bulk density of the granular material. Herein, the two densities are connected by the porosity *n* of the granular material, viz.:

$$\rho^{\text{bulk}} = n\, \rho^{\text{particle}}\,. \tag{3}$$

The question of which one to choose from is of rather practical nature and mainly depends on the available computational power. Recalling the previously mentioned scales, it is often impossible to actually capture each and every grain. Thus, a coarse-graining technique (often also known as "upscaling") needs to be applied.

If the computing power is big enough to capture the actual particles, the particle mass *M* or particle density ρ^{particle} needs to be measured and prescribed. For spherical particles, the radius *r* is also simply measured, while for non-spherical particles some sort of spherical approximation needs to be carried out. Herein, several methods exist that define the radius to obtain a sphere with the maximum/minimum length, same surface area, same volume, same weight, same surface-to-volume ratio of the non-spherical particle or to obtain a sphere that passes the same sieve aperture, etc.

If, however, the compute power is not big enough (which is usually the case), a homogenization scheme needs to be applied. Herein, the first assumption to be made addresses the amount of coarse graining to be applied, i. e., how many small particles of the real-scale problem are replaced by a single bigger rigid sphere to allow a numerical treatment of the overall particle system, cf. Figure 4.

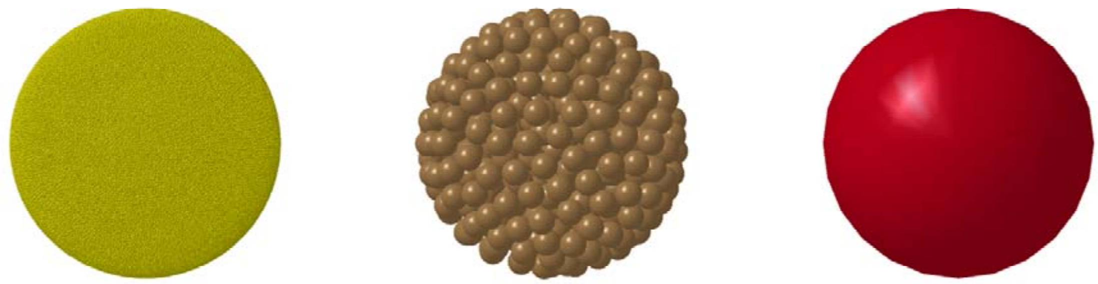

546 820 spheres @ r_{real} = 0.05   491 spheres @ r_{real} = 0.5   1 sphere @ r_{coarse} = 5.0

Fig. 4: Coarse-graining of several small spheres with radii r_{real}=0.05 or r_{real}=0.5 with respective particle density ρ^{particle} to a single particle with radius r_{coarse}=5.0 and bulk density ρ^{bulk}.

Note that the amount of coarse-graining that needs to be applied to a granular system is a problem-specific constitutive decision. For hopper flows for example, it is good practice to introduce a characteristic length scale *D* of the hopper, e. g., the diameter of the outlet. This will lead to a characteristic scale number

$$S_n = \frac{D}{r} \ , \tag{4}$$

which relates the characteristic length *D* of the granular system to the chosen coarse-grained particle radius *r*. Good modeling practice proceeds with a scale number $S_n \geq 10$, such that at least 5 particles aligned perpendicular to the outflow can pass through simultaneously. More information on scale numbers and the associated similarity investigations of coarse-grained systems can be found in [3], where the author uses the term "upscaling" instead of coarse graining.

Things to keep in mind

The bulk behavior of the granular material will be influenced by the size distribution of the particles. Non-spherical particles introduce additional moments due to the possible offset of contact forces, which can be accounted for by introducing a rolling friction. Coarse-graining will approximate a deformable cluster of particles with a single rigid sphere. Thus, the dissipated frictional energy inside the cluster of particles during deformation needs to be captured via the contact law for particle-particle interaction.

Definition of the Particle-Particle Interaction

Associated keywords

The penalty-based particle-particle interaction is defined using the keyword **`*CONTROL_DISCRETE_ELEMENT`**, which provides the possibility to define normal and tangential stiffness and damping coefficients, static friction and rolling friction coefficients, as well as a liquid surface tension to account for capillary forces between wet particles, cf. Figure 3a). For the sake of simplicity, the case of wet particles will not be treated here in more detail.

```
*CONTROL_DISCRETE_ELEMENT
$#--+----1----+----2----+----3----+----4----+----5----+----6----+----7----+----8
$#    NDAMP     TDAMP      Fric     FricR     NormK    ShearK       CAP     MXNSC
      0.700     0.400      0.41     0.001      0.01    0.0029         0         0
$#    Gamma    CAPVOL    CAPANG
       26.4      0.66      10.0
```

Associated parameters for the penalty stiffness

The first quantity that influences the mechanical penalty-based particle-particle contact is the elastic stiffness of the spring elements. Herein, the normal contact force contribution is given by

$$F_n = K_n\, d_{\text{int}} \quad \text{with} \quad K_n = \begin{cases} \frac{\kappa_1 r_1 \kappa_2 r_2}{\kappa_1 r_1 + \kappa_2 r_2}\texttt{NormK} & : \text{if } \texttt{NormK} > 0 \\ |\texttt{NormK}| & : \text{if } \texttt{NormK} < 0 \end{cases} \quad \text{and} \quad \kappa = \frac{E}{3(1-2\nu)}, \tag{5}$$

where κ_i are the compression moduli of two neighboring spheres that are computed by LS-DYNA using the Young's modulus E and the Poisson ratio ν given in **`*MAT_ELASTIC`.** Setting the parameter `NormK` to values greater than zero allows to scale a penalty stiffness, which depends on the compression moduli and the radii of two contacting spheres, thus leading to a length-scale invariant formulation. If, for any reason, the contact stiffness needs to be directly prescribed, it can be achieved by setting `NormK` to a value less than zero.

Note that the tangential spring constant is given relative to the normal spring constant using $K_t = K_n\,\texttt{ShearK}$. Suggested default values for `NormK` and `ShearK` are 0.01 and $\frac{2}{7} = 0.2857$, respectively. Herein, an analogy can be drawn between continuum and granular mechanics that interprets the ratio K_t/K_n as Poisson's ratio, cf. Table 1.

Continuum model		DEM system	
Young's modulus E, compression modulus $\boldsymbol{\kappa}$	[Pa]	K_n	[N/m]
Poisson's ratio $\boldsymbol{\nu}$	[-]	$\frac{K_t}{K_n}$	[-]

Table 1 Parameter analogy between continuum models and DEM systems.

Regarding the definition of the elastic constants E and ν there exist again two scenarios. In rare cases, where the actual particle size is modeled, the elastic constants can be directly measured with the aid of an indentation test or a similar experimental procedure.

If a coarse-graining procedure has been applied, which is the usual case in process engineering and materials handling, the elastic constants represent the bulk behavior of the underlying sum of particles as is shown in Figure 4. In this case, it is not possible to directly measure the elastic constants with an experiment. Instead, experiments capturing the bulk behavior of many particles need to be performed and simulations of the same experiment with coarse-grained spheres need to be computed to fit the elastic constants of the contact law. One suitable experiment among others is a biaxial test with a rectangular specimen, where pressure is applied to the side surfaces, back, front and bottom surfaces are fixed and the top surface is moved downwards, cf. Figure 5a. Herein, the required force is measured to prescribe a displacement on the top surface, which is then compared to a numerical simulation with coarse-grained spheres. Note that the elastic constants mostly influence the elastic region as indicated in Figure 5b.

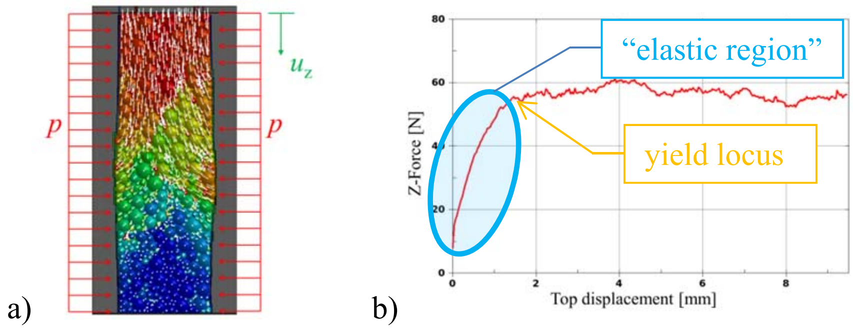

Fig. 5: a) Setup of a biaxial test with prescribed horizontal pressure p and top displacement u_z and b) measurement of the bulk behavior in terms of a force-displacement diagram with indicated "elastic region" and yield locus to indicate the violation of the static friction law.

Things to keep in mind

If the granular system is used for geotechnical applications, the measurement of the elastic constants is crucial to obtain the correct base-failure behavior. However, in many industrial applications, the elastic constants do not play the most important role, as the deformations associated with the overlap of the penalty-contact are small compared to the relative motion a particle undergoes on a conveyor belt.

Moreover, the elastic stiffness of the penalty contact K_n is directly associated with the critical timestep, i. e., the stiffer the contact law, the smaller the timestep. Thus, it can be also worth scaling the penalty contact stiffness `NormK` down by a factor of 100 or more to reach a bigger timestep, which in turn allows for the treatment of even bigger particle assemblies [4]. Even though one loses accuracy in the elastic bulk behavior, the accuracy gain due to the ability to compute larger particle systems might be more beneficial.

Associated parameters for the coefficient of restitution

In LS-DYNA, the coefficient of restitution during particle-particle contact as well as particle-wall contact is enforced by applying a fraction of the critical damping force. Herein, the contribution in normal direction reads:

$$F_n = D_n \dot{d}_{\text{int}} \ . \qquad (6)$$

The parameters `NDAMP` and `TDAMP` define the coefficient of restitution which is used as the ratio of the critical damping in the normal and tangential directions, respectively, yielding

$$D_{n/t} = \mathsf{DAMP}\ \eta_{\text{crit}} = 2.0\ \mathsf{DAMP} \sqrt{\frac{m_1 m_2}{m_1+m_2} K_{n/t}} \qquad \text{with} \qquad 0 \leq \mathsf{DAMP} \leq 1.0 \ . \qquad (7)$$

Figure 6 shows the influence of the normal damping on a particle that is dropped onto another particle from 1m height under gravity loading.

Again, the experimental determination of the coefficient of restitution by measuring the rebound height is only possible in rare cases where the actual particle size is modeled. For coarse-grained particle systems it is again not possible to directly measure the coefficient of restitution. In fact, even with bulk experiments, it is hard to achieve. However, in many industrial applications, the coefficient of restitution is set to a relatively high level between 0.5 and 0.9.

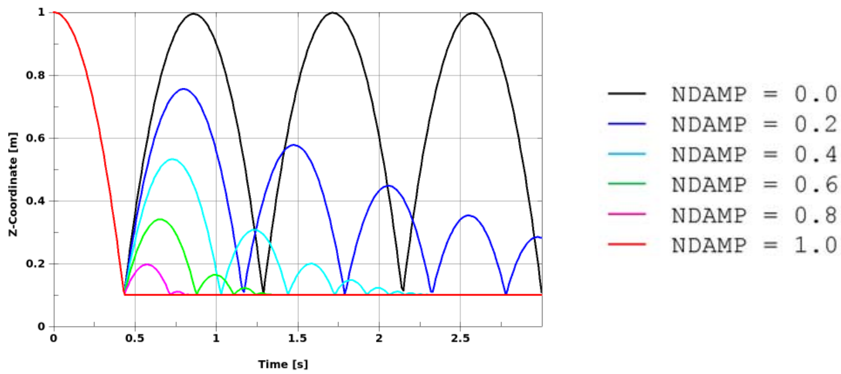

Fig 6: Influence of the normal damping during particle-particle contact resulting from a drop under gravity loading from a height of 1m.

Things to keep in mind

In coarse-grained systems, the coefficient of restitution is a workaround to account for the internal dissipation inside a coarse-grained "macro" sphere due to friction. Thus, it has nothing to do with the coefficient of restitution of a single solid spherical particle. Figure 7 shows what would happen during the impact of a coarse-grained "macro" sphere. The simulation is carried out to achieve a fully plastic impact of a sphere that was modeled using a thin rubber coating filled with several rigid "micro" spheres. Herein, all energy of the impact is dissipated by friction between the "micro" spheres. To capture this behavior with a single coarse-grained sphere, a coefficient of restitution equal to unity needs to be prescribed via `NDAMP`.

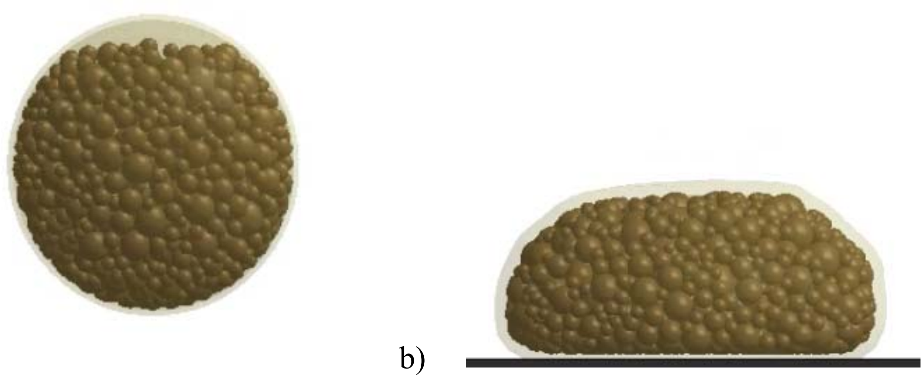

a) b)

Fig 6: Droptest of a coarse-grained spherical particle just before impact (a) and after impact (b). All energy is dissipated by internal friction between the "micro" particles.

Associated parameters for static and rolling friction

The remaining parameters are needed to quantify the internal friction of granular media and are thus a key enabler to correctly model the flow properties of granular particle systems. However, if a coarse-graining procedure was prescribed, the identification of the correct parameters is not an easy task, as the needed bulk parameters are a result of many effects occurring on the micro scale, cf. Figure 6. In particular, the real friction parameters of the micro spheres as well as particle shape and size distribution or packing density have an influence on the bulk coefficients.

In LS-DYNA, the frictional force component F_{fr} of the mechanical particle-particle contact is based on Coulombs law of dry friction

$$F_{fr} \leq \mu_{fr} F_n \ , \tag{8}$$

which depends on the coefficient of dry friction μ_{fr} (`Fric`) and the sum of all normal forces F_n given in (5) and (6). The same law of static friction is used for the particle-wall contact which is characterized in **`*DEFINE_DE_TO_SURFACE_COUPLING.`** Subsequently, the two static friction coefficients μ_{fr}^{p-p} and μ_{fr}^{p-w} receive an extra superscript to indicate the particle-particle and particle-wall contact, respectively, wherever necessary.

Note that a vanishing friction coefficient yields a central force system for each particle and thus, LS-DYNA reduces the degrees of freedom (DOF) of each spherical particle to three translations. Moreover, only friction coefficients greater than zero allow tangential friction forces to be induced at the perimeter of a spherical particle and thus, yield a general force system and the need for six DOF per spherical particle in LS-DYNA, i. e., three translations and three rotations.

To account for a certain surface roughness of the spherical particles or even to approximate other particle shapes like the ones indicated in Figure 2, the DEM in LS-DYNA is extended by the introduction of a rolling resistance `FricR`. Typical values for sand grains are around `FricR` = `0.01`, depending on the smoothness of the grains. For the particle-wall contact the rolling friction is defined via `FricR` in **`*DEFINE_DE_TO_SURFACE_COUPLING.`** Following this, a moment M_r is introduced similar to (8) that tends to retard the rolling motion, viz.:

$$M_r = r \ \mu_{roll} \ F_n \ . \tag{9}$$

Again, the coefficient of rolling friction μ_{roll} will be equipped with a superscript when needed.

A first impression of μ_{fr}^{p-p} is received by identifying the onset of a yield locus in a biaxial test, cf. Figure 5b. At this loading state, the law of static friction (8) is violated and shear bands start to evolve where the particles within the shear band perform a rolling motion. Thus, the biaxial test is in principle suitable to identify the coefficients of static friction μ_{fr}^{p-p} and rolling friction μ_{roll}^{p-p}. However, this is only a very common test in the geo-technical community, as the elastic constants need to be determined exactly.

In process engineering and materials handling, different experiments are often performed to identify the friction parameters. In particular, these experiments are direct shear tests using a shear cell or a rotary drum as well as flow tests by measuring hopper flow or pile formation tests. Following [4], it is of great importance to perform at least two of these tests, as the coefficients of static and rolling friction are often coupled.

For example, when the granular material is tested in a shear cell, there exist a variety of combinations for the coefficients of static friction μ_{fr}^{p-p} and rolling friction μ_{roll}^{p-p} that reproduce the bulk behavior of the experiment, i.e., the measured shearing force of the shear cell [4]. Following this, the two parameters are not clearly identified by a single experiment. Thus, it is highly recommended to perform a second experiment where the friction parameters μ_{fr}^{p-p} and μ_{roll}^{p-p} can be fitted to match the bulk behavior. In [4], the second experiment was the investigation of the angle of repose in a rotary drum, which is supposed to exhibit the same ambiguity as the shear cell. In combination, it should be possible to find matching pairs for the friction parameters μ_{fr}^{p-p} and μ_{roll}^{p-p} in both experiments.

An example how it should not be done to identify the particle-particle friction coefficients is shown in Figure 7. Herein, the rotary speed was set too fast such that there is no pure rolling motion of the particles induced. Instead, the rotary drum transports the particles too fast, such that a frequent change between a cascading and a cateracting motion can be observed. This makes it very hard to measure the angle of repose. However, note that rotary drums with a higher rotation speed tend to be influenced more by the particle-wall friction coefficients, which might be of interest when identifying these parameters.

Fig 7: Rotary drum experiment with motion forms changing between cascading and cateracting modes showing a changing angle of repose α.

Things to keep in mind

As the introduction of a rolling friction is only a workaround, this might not be sufficient for really non-spherical particle systems.

References

[1] Karajan, N.; Han, Z.; Ten, H. and Wang, J.: Interaction Possibilities of Bonded and Loose Particles in LS-DYNA. *Proceedings of the 9th European LS-DYNA Conference*, Manchester, 2013

[2] Cundall, P. A. and Strack, O. D. L.: A discrete numerical model for granular assemblies. *Geotechnique* **29** (1979), 47–65

[3] Feng, Y.T.; Han, K. and Owen, D.R.J.: On upscaling of discrete element models: Similarity principles. *Engineering Computations: International Journal for Computer-Aided Engineering and Software* **26** (2009), 599–609

[4] Gröger T. and Katterfeld A.: On the numerical calibration of discrete element models for the simulation of bulk solids. *Proceedings of the 16th European Symposium on Computer-Aided Process Engineering and 9th International Symposium on Process Systems Engineering* (2006), 533–538